International Journal of Innovative Research in Computer and Communication Engineering

| e-ISSN: 2320-9801, p-ISSN: 2320-9798| www.ijircce.com | Impact Factor: 7.194 |

|| Volume 8, Issue 4, April 2020 ||

Medical Image Mixed Denoising Using Improved K-VSD Algorithm Based Discrete Wavelet Novel Threshold Method

Mr.Yared Abera Ergu[1], Mr.Gaddisa Hailu[2], Dr.S. Kother Mohideen[3]

Dean, School of Technology & Informatics, Ambo University, Woliso Campus ,Ethiopia[1]

Head of the Department, Department of Information System , Ambo University, Woliso Campus, Ethiopia[2]

Professor, Department of Information System ,Ambo University, Woliso Campus, Ethiopia[3]

ABSTRACT: The image de-noising naturally corrupted by noise is a classical problem in the field of signal or image processing. Additive random noise can easily be removed using simple threshold methods. De-noising of medical images in Magnetic Resonance Images (MRI) corrupted by Gaussian noise and Rician noise Mixture using wavelet techniques are very effective because of its ability to capture the energy of a signal in few energy transform values. MRI imaging creates a distinctive view into the interior of a human body and has become an essential tool of clinical diagnosis. However, Rician and Guasian noise mixed is a type of artifact inherent to the acquisition process of the magnitude MRI image, making diagnosis difficult. We proposed moment based Gaussian Rician mixture noise reduction technique decompose the image using discrete wavelet and then applied Improved K-SVD algorithm and novel threshold for mixed noise removal. The proposed method can efficiently remove a variety of mixed or single noise while preserving the medical image information well. It is proposed to investigate the suitability of different wavelet bases and the size of different neighborhood on the performance of image de-noising algorithms in terms of PSNR. The experimental results demonstrate Our proposed scheme shows better results against various quality measures in terms of noise removal and edge preservation while retaining fine image information compare with high end existing methods.

KEYWORDS: MRI (Magnetic Resonance Images),PSNR, Denoising, K-SVD,Gaussian Noise, Rician Noise Additive random noise.

I INTRODUCTION

Image denoising is a method of removal of noise while retaining as much as possible important information. It is the method of producing a good estimate of the original image from noisy observations. There are two basic approaches to image denoising, namely spatial filtering methods and transform filtering methods. Spatial Filtering methods try to remove the noise by manipulating the image in the spatial domain itself whereas transform filtering methods are using some transform to manipulate the image in transform domain. In transform domain, Wavelets give a superior performance in image denoising due to its properties such as sparsity, energy compaction and multi-resolution structure. So, the focus was shifted from the spatial and Fourier domain to the wavelet transform domain. In wavelet transform, the small coefficients are more likely due to noise and large coefficients are more likely due to important feature of the image. These small coefficients can be thresholded without affecting the significant features of the image. Thresholding is a simple non-linear technique, which operates on one wavelet coefficient at a time. In its most basic form, each coefficient is thresholded by comparing against threshold, if the coefficient is smaller than threshold, set to zero; otherwise it is kept or modified. Replacing the small noisy coefficients by zero and inverse wavelet transform on the result may lead to reconstruction with the essential signal characteristics and with less noise. . But, wavelet transform suffers due to poor directionality and does not provide a geometrically oriented decomposition in multiple directions. One way to generalize the discrete wavelet transform so as to generate a structured dictionary of base is given by the Discrete Wavelet Packet Transform (DWPT). This benefit comes from the ability of the wavelet packets to better represent high frequency content and high frequency oscillating signals in particular. However, it is well known that both DWT and DWPT are shift varying. The Dual Tree Complex Wavelet Transform (DTCWT) introduced by Kingsbury is approximately shift -invariant and provides directional analysis. In this paper, it is proposed to combine two thresholding techniques namely Neighshrink and Sureshrink to

| e-ISSN: 2320-9801, p-ISSN: 2320-9798| www.ijircce.com | Impact Factor: 7.194 |

|| Volume 8, Issue 4, April 2020 ||

denoise an image corrupted by additive white Gaussian noise using DTCWT and the performance of DTCWT for the denoising of images are evaluated using RMSE and PSNR.

II DISCRETE WAVELET TRANSFORM

Wavelet transforms provide a framework in which a signal is decomposed, with each level corresponding to a coarser resolution, or lower frequency band[27]. There are two main groups of transforms, continuous and discrete. Discrete transforms are more commonly used and can be subdivided in various categories. Although a review of the literature produces a number of different names and approaches for wavelet transformations, most fall into one of the following three categories: decimated, un-decimated, and non-separated. A continuous wavelet transform is performed by applying an inner product to the signal and the wavelet functions. The dilation and translation factors are elements of the real line. For a particular dilation a and translation b, the wavelet coefficient W_f (a,b) for a signal f can be calculated as

$$W_f(a,b) = \langle f, \psi_{a,b} \rangle = \int f(x)\psi_{a,b}(x)dx \qquad (1)$$

Wavelet coefficients represent the information contained in a signal at the corresponding dilation and translation. The original signal can be reconstructed by applying the inverse transform:

$$f(x) = c\frac{1}{w}\int_{-\infty}^{\infty}\int_{-\infty}^{\infty} W_f\ (a,b)\psi_{a,b}(x)\ db\ \frac{da}{a^2} \qquad (2)$$

where Cψ is the normalization factor of the mother wavelet. Although the continuous wavelet transform is simple to describe mathematically, both the signal and the wavelet function must have closed forms, making it difficult or impractical to apply. The discrete wavelet is used instead. The term discrete wavelet transform (DWT) is a general term, encompassing several different methods. It must be noted that the signal itself is continuous; discrete refers to discrete sets of dilation and translation factors and discrete sampling of the signal[27]. For simplicity, it will be assumed that the dilation and translation factors are chosen so as to have dyadic sampling, but the concepts can be extended to other choices of factors. At a given scale J, a finite number of translations are used in applying multi resolution analysis to obtain a finite number of scaling and wavelet coefficients. The signal can be represented in terms of these coefficients as

$$f(x) = \sum_k C_{jk}\phi_{jk}(x) + \sum_{j=1}^{j}\sum_k d_{jk}\psi_{jk}(x) \qquad (3)$$

where $c_{Jk}$are the scaling coefficients and djk are the wavelet coefficients. The first term in Eq. (3) gives the low-resolution approximation of the signal while the second term gives the detailed information at resolutions from the original down to the current resolution J. The process of applying the DWT can be represented as a bank of filters, as in figure 4. In case of a 2D image, a single level decomposition can be performed resulting in four different frequency bands namely LL, LH, HL and HH sub band and an N level decomposition can be performed resulting in 3N+1 different frequency bands and it is shown in figure 1. At each level of decomposition, the image is split into high frequency and low frequency components; the low frequency components can be further decomposed until the desired resolution is reached. When multiple levels of decomposition are applied, the process is referred to as multi-resolution decomposition. In practice when wavelet decomposition is used for image fusion, one level of decomposition can be sufficient, but this depends on the ratio of the spatial resolutions of the images being fused.

| e-ISSN: 2320-9801, p-ISSN: 2320-9798| www.ijircce.com | Impact Factor: 7.194 |

|| Volume 8, Issue 4, April 2020 ||

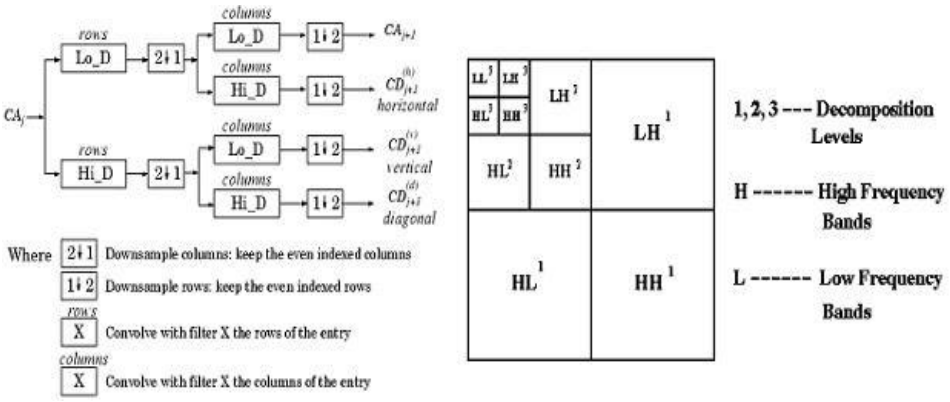

Fig.1: 2D-Discrete Wavelet Transform

The conventional DWT can be applied using either a decimated or an un-decimated algorithm. In the decimated algorithm, the signal is down sampled after each level of transformation. In the case of a two-dimensional image, down-sampling is performed by keeping one out of every two rows and columns, making the transformed image one quarter of the original size and half the original resolution. The decimated algorithm can therefore be represented visually as a pyramid, where the spatial resolution becomes coarser as the image becomes smaller. The decimated algorithm is not shift-invariant, which means that it is sensitive to shifts of the input image. The decimation process also has a negative impact on the linear continuity of spatial features that do not have a horizontal or vertical orientation. These two factors tend to introduce artifacts when the algorithm is used in applications such as image denoising.

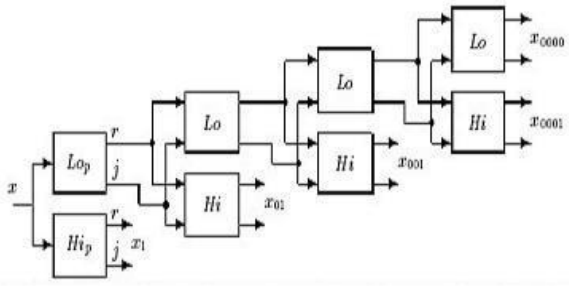

Fig .2 Four levels of Complex Wavelet Tree for real 1-D input signal x

Extension of complex wavelets to 2-D is achieved by separable filtering along rows and then columns. However, if row and column filters both suppress negative frequencies, then only the first quadrant of the 2-D signal spectrum is retained. Two adjacent quadrants of the spectrum are required to represent fully a real 2-d signal, so we also need to filter with complex conjugates of either the row or column filters. This gives 4:1 redundancy in the transformed 2-D signal. If the signal exists in m-d (m > 2), then further conjugate pairs of filters are needed for each dimension leading to redundancy of 2^m:1. The most computationally efficient way to achieve the pairs of conjugate filters is to maintain separate imaginary operators, j_1 and j_2, for the row and column processing, as shown in figure 6. This produces 4-element `complex' vectors: {r, $j_1$, $j_2$, $j_1j_2$} (where r means `real'). Each 4-vector can be converted into a pair of conventional complex 2-vectors, by letting $j_1 = j_2 = j$ in one case and $j_1 = -j_2 = -j$ in the other case. This corresponds to sum and difference operations on the {r, j_1j_2} and {j_1,j_2} pairs in the summation blocks in figure 6 and produces two complex outputs, corresponding to first and second quadrant directional filters respectively. Complex filters in multiple dimensions provide true directional selectivity, despite being implemented separably, because they are still able to separate all parts of the m-D frequency space. For example a 2D DTCWT produces six band pass sub-images of complex coefficients at each level, which are strongly oriented at angles of ± 15°, ± 45°, ± 75°, shown by the double-headed arrows in figure 6. The DTCWT consists of two wavelet transforms operating in parallel on an input signal as illustrated in Figure 7. We denote the wavelet associated with the first wavelet filter bank as □(t) and the wavelet associated with the second filter bank as □'(t). The wavelet □(t) is defined by

| e-ISSN: 2320-9801, p-ISSN: 2320-9798| www.ijircce.com | Impact Factor: 7.194 |

|| Volume 8, Issue 4, April 2020 ||

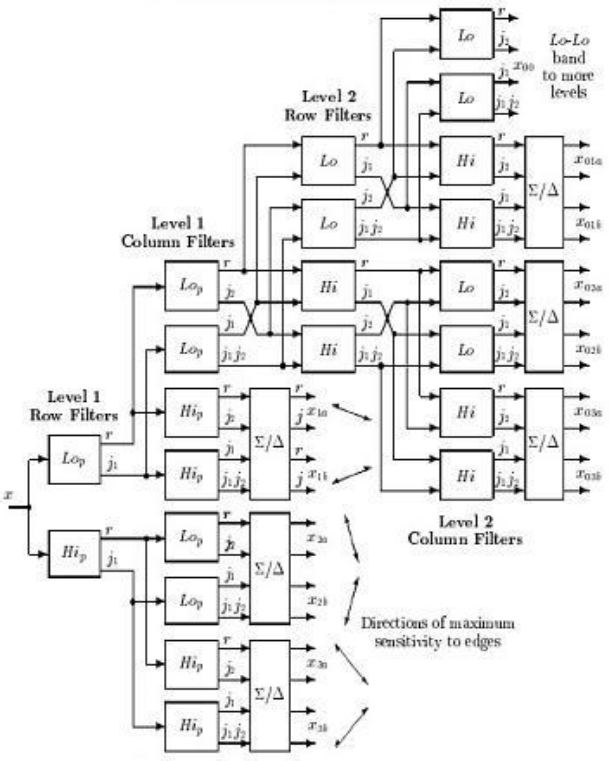

Fig3 Two levels of the Complex Wavelet tree for a real 2-D input image x giving 6 directional bands

$$\phi(t) = \sqrt{2}\sum_n h_0(n)\phi(2t-n).$$

The second wavelet, □' (t), is defined similarly in terms of {h'$_0$(n), h'$_1$(n)}. For the ideal DT-CWT, the second wavelet, □'(t), is the Hilbert transform of the first wavelet,□ (t),

$$\acute{\psi}(t) = H\{\psi(t)\} \quad (5)$$

If the low-pass filter h'$_0$(n) is equal to the half-sample delayed version of h$_0$(n), then the wavelets generated by the DTCWT satisfy as desired. If the given wavelets, □(t) and □'(t), are orthogonal to its integer translates, then the Hilbert relation is satisfied if and only if ,

$$H_0^1(e^{jw}) = e^{-j0.5w}H_0(e^{jw}) for\ |W| \langle \pi \quad (6)$$

Recall that for an orthonormal wavelet basis, the lowpass and high-pass filters are related as

$$F\left(e_1^{jw}\right) = -e^{-jdw}H_0^1(e^{j(w-\pi)}) \quad (7)$$

equivalently h$_1$(n)=(-1)^{n}h$_0$(d-n), where 'd' is an odd integer. Hence, it follows from that for the ideal DT-CWT, the high-pass filters satisfy

$$H_1^1(e^{jw}) = -sgn(w)e^{j\,0.5\,w}H_1(e^{jw}) for\ |W| \langle \pi \quad (8)$$

| e-ISSN: 2320-9801, p-ISSN: 2320-9798| www.ijircce.com | Impact Factor: 7.194 |

|| Volume 8, Issue 4, April 2020 ||

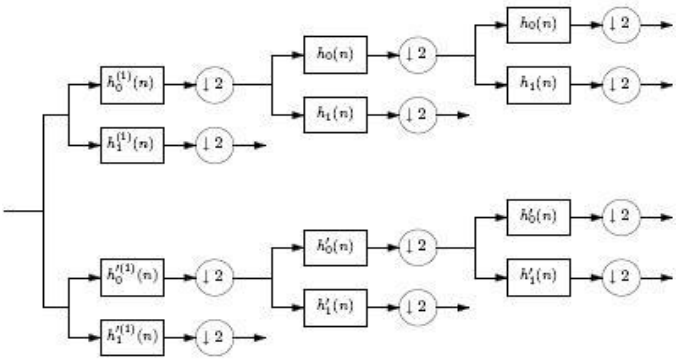

Fig 4: Implementation of DTCWT using Two Wavelet Filters

III WAVELET BASED IMAGE DENOISING

All digital images contain some degree of noise. Image denoising algorithm attempts to remove this noise from the image. Ideally, the resulting de-noised image will not contain any noise or added artifacts. De-noising of natural images corrupted by Gaussian noise using wavelet techniques is very effective because of its ability to capture the energy of a signal in few energy transform values.

Here, the threshold plays an important role in the denoising process. Finding an optimum threshold is a tedious process. A small threshold value will retain the noisy coefficients whereas a large threshold value leads to the loss of coefficients that carry image signal details. Normally, hard thresholding and soft thresholding techniques are used for such de-noising process. Hard thresholding is a keep or kill rule whereas soft thresholding shrinks the coefficients above the threshold in absolute value. It is a shrink or kill rule.

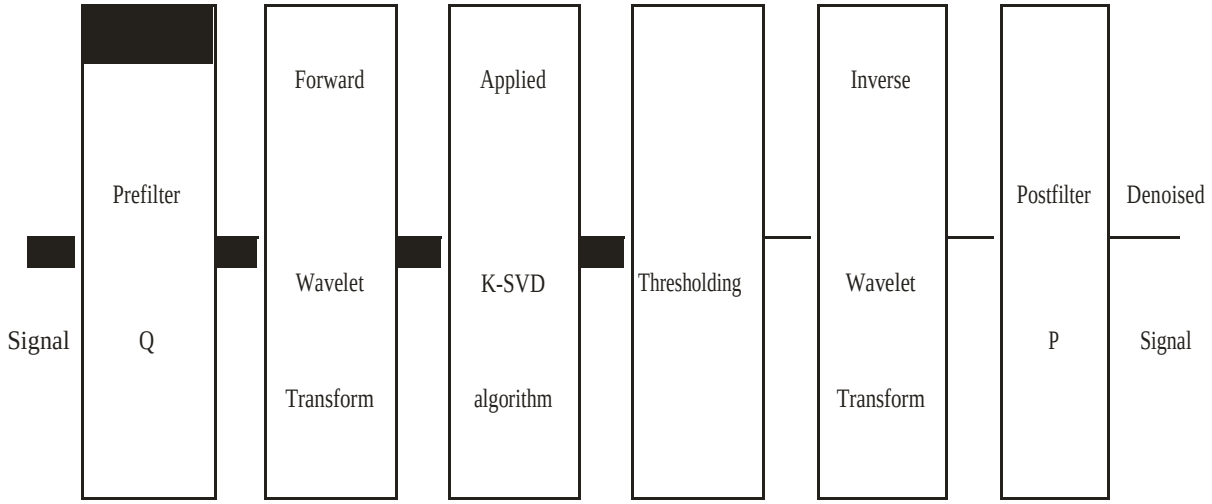

Fig 5. Diagram of wavelet based image De-noising

Improved K-SVD Denoising Algorithm:

The K-SVD algorithm will be built upon sparse representations[28], now the brief review the main mathematical ideas of the K-SVD denoising algorithm. Let g, f ∈ R$S1 \times S2$ be the $S1 \times S2$ size noisy and clean images, respectively. To simplify

| e-ISSN: 2320-9801, p-ISSN: 2320-9798| www.ijircce.com | Impact Factor: 7.194 |

|| Volume 8, Issue 4, April 2020 ||

notations, here always use the lowercase letters such as $g \in RS1S2$ to represent a column vector by stacking the columns of the matrix g. According to the maximum a-posteriori probability (MAP) estimator and an assumption that each small image patch can be sparsely represented as a linear combination of a redundant learned dictionary.
The following steps for the K-SVD algorithm

- Select atoms from input
- Atoms can be patches from the image
- Patches are overlapping
- Replace unused atom with minimally represented signal
- Identify signals that use *k*-th atom (non zero entries in rows of **X**)
- Deselect *k*-th atom from dictionary
- Find coding error matrix of these signals
- Minimize this error matrix with rank-1 approximate from SVD

The above steps are repeated until the path can be sparsely represent for entire image

Probability Density Functions of Mixed Noise

Here Gaussian and Rician mixed noise removal via energy minimization method. For real images, the probability density function (PDF) is often not a single standardized distribution such as Gaussian[28]. Thus its MLE is often difficult to solve. Here we consider the case that the noise is sampled from several different distributions. This mixed noise in images is more difficult to remove than the standardized Gaussian noise. And also described the framework for restoring images corrupted by mixed noise.
Suppose the mixed noise $n \in RS1S2$ is constituted by M different groups nl , $l = 1, 2, \ldots, M$, each sl is some realizations of a random variable Sl with PDF $pl(x)$, and the ratio of each $s1$ is rl. Here rl satisfies_M l=1 rl = 1. Similarly, s can also be regarded as some realizations of a random variable N whose PDF is $p(x)$. With these assumptions, one can get the PDF of mixed noise

$$p(x) = M\_l=1 rl\ pl(x) \qquad \ldots\ldots\ldots (9)$$

VisuShrink

VisuShrink is thresholding by applying the Universal threshold proposed by Donoho and Johnstone. This threshold is given by $\sigma^2 \log M$ where σ is the noise variance and M is the number of pixels in the image. It is proved that the maximum of any M values iid as $N(0,\sigma^2)$ will be smaller than the universal threshold with high probability, with the probability approaching 1 as M increases. Thus, with high probability, a pure noise signal is estimated as being identically zero.

Bayesshrink

BayesShrink is an adaptive data-driven threshold for image denoising via wavelet soft-thresholding. The threshold is driven in a Bayesian framework and assumed generalized Gaussian distribution (GGD) for the wavelet coefficients in each detail subband and try to find the threshold T which minimizes the Bayesian Risk.

Neighshrink

For each noisy wavelet coefficient $W_{i,j}$ to be shrinked, it incorporates a square neighbouring window B_{ij} centered at it. The neighbouring window size can be represented as LXL, where L is a positive odd number. The Neighshrink shrinkage formula can be represented as

$$S2 = \sum k, I \varepsilon B \quad W \quad 2$$

$$i,j \qquad\qquad i,j \quad kl$$

(10)

$$\bar{[2]} \qquad i,j = Wi,j\ Bi,j$$

| e-ISSN: 2320-9801, p-ISSN: 2320-9798| www.ijircce.com | Impact Factor: 7.194 |

|| Volume 8, Issue 4, April 2020 ||

$$\bar{[2]} \qquad i, j \square Wi, j Bi, j$$

where $\square i, j$ is the estimator of the unknown noiseless coefficient, and λ is the universal threshold. (g) is defined as (g) = max (g,0). Different wavelet coefficient subbands are shrinked independently, but the threshold λ and neighbouring window size L keep unchanged in all subbands. When $S_{i,j}^2$ summation has pixel indexes out of the wavelet subband range, the corresponding terms in the summation are omitted. The shortcoming of this method is that using the same universal threshold λ and neighbouring window size L in all subbands is suboptimal.

SureShrink

SureShrink is a thresholding technique in which adaptive threshold is applied to subband, a separate threshold is computed for each detail subband based upon SURE (Stein's unbiased estimator for risk), a method for estimating the loss in an unbiased fashion. The optimal λ and L of every subband should be data-driven and minimize the mean squared error (MSE) or risk of the corresponding subband. Fortunately, Stein has stated that the MSE can be estimated unbiasedly from the observed data. NeighShrink can be improved by determining an optimal threshold and neighbouring window size for every wavelet subband using the Stein's unbiased risk estimate (SURE). For ease of notation, the Nsnoisy wavelet coefficients from subband 's' can be arranged into the 1-D vector. Similarly, we combine the Ns unknown noiseless coefficients from

for almost any fixed estimator θ_S based on the data w_S, the expected loss (i.e. risk) $E\left\{\left\|\bar{\theta}s-\theta\right\|_2^2\right\}$ can be estimated unbiasedly. Usually, the noise standard deviation σ is set at 1, and then

$$E\left\{\left\|\bar{\theta}s-\theta s\right\|_2^2\right\} = -N_s + E\left\{\left\|g(w_s)\right\|_2^2 + 2\nabla.g(w_s)\right\} \qquad (11)$$

Neighsureshrink

The quantity

$$SURE(w_S, \lambda, L) = N_S + \sum_n \left\|g_n(w_n)\right\|_2^2 + 2\sum_n \frac{\partial g_n}{\partial n} \qquad (12)$$

is an unbiased estimate of the risk on subband s where L is the neighbourhood window size (L is an odd number and greater than 1, for example, 3, 5, 7, 9, etc.): $E\left\{\left\|\bar{\theta}s-\theta\right\|_2^2\right\} = E\{SURE(w_s, \lambda, L\}$. Then, it can be choosen the threshold λ^s and neighbouring window size L^s on subband 's' which minimizes SURE(w_s, λ, L).

subband 's' into the corresponding 1-D vector. Stein shows that,

IV RESULTS AND DISCUSSIONS

For the above mentioned Wavelet and novel Threshold Method , image de-noising is performed using wavelets from the second level to fourth level decomposition and the results are shown in figures and table if formulated for second level decomposition for different noise variance as follows. It was found that three level decomposition and fourth level decomposition gave optimum results.

However, third and fourth level decomposition resulted in more blurring. The experiments were done using a window size of 3X3, 5X5 and 7X7 for Novel wavelet Threshold Method . The neighborhood window of 3X3 and 5X5 are good choices for mammographic images The images are taken from MIAS database.

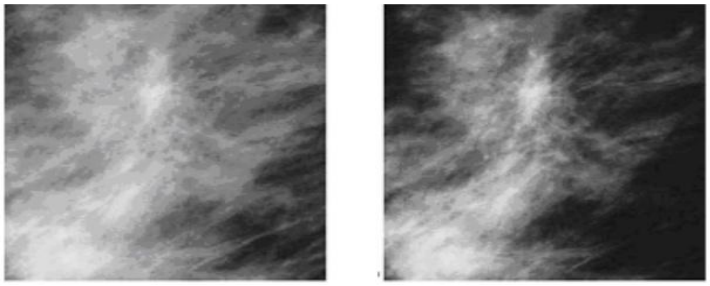

Fig 6 Original Noise MRI Brest Cancer Mammogram Images

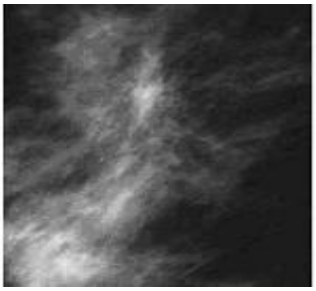

Fig.7 After Apply K-VSD Algorothm MRI Images

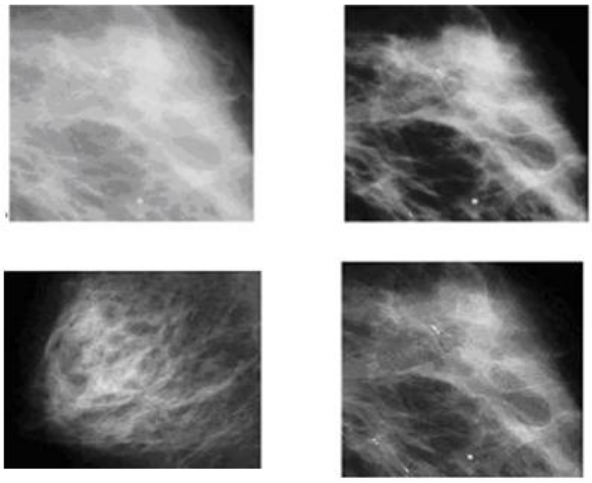

Fig8 After Applied Wavelet Threshold Method (Denoised MRI Mammagram Images)

Window Size		3X3				5X5				7X7			
Wavelet	Variance	0.02	0.04	0.06	0.08	0.02	0.04	0.06	0.08	0.02	0.04	0.06	0.08
	Noisy Image	16.8601	14.1096	12.6435	11.6742	16.8309	14.0995	12.6717	11.681	16.8464	14.103	12.64	11.6592
	Wiener	24.056	21.343	19.9475	19.0223	26.4167	24.1466	22.8984	21.98	26.6335	24.8262	23.732	22.9097
Harr	Visushrink	22.2984	19.7787	18.3776	17.3849	22.2735	19.7681	18.3769	17.431	22.2856	19.807	18.332	17.4044
	Neighshrink	24.5738	23.3066	22.2924	21.5432	24.5822	23.2459	22.3749	21.555	24.5573	23.254	22.287	21.5715

	Mod.Nei	25.961	25.0158	24.1295	23.4049	25.9627	24.9922	24.2039	23.438	25.9578	24.988	24.093	23.3887
	Proposed K-VSD Wavlet	26.87	26.044	25.2441	24.966	27.189	26.733	26.1236	25.111	27.3468	26.877	25.879	25.0014
db 16	Visushrink	22.6224	20.0023	18.4513	17.5362	22.6177	19.9746	18.4704	17.506	22.6147	19.97	18.508	17.5385
	Neighshrink	23.3646	22..3845	21.5909	21.0162	23.3556	22.4143	21.6199	21.04	23.366	22.359	21.629	21.0237
	Mod.Nei	24.332	23.7027	23.0889	22.5978	24.3175	23.7657	23.1492	22.627	24.3335	23.681	23.129	22.5932
	Proposed K-VSD Wavlet elet	25.412	24.9421	24.6012	24.015	25.4561	24.9455	24.4588	24.104	25.4563	24.978	24.459	23.894
Sym 8	Visushrink	22.6042	19.9785	18.5036	17.4728	22.5682	19.9576	18.5172	17.517	22.6058	19.984	18.454	17.4988
	Neighshrink	23.4209	22.5088	21.6579	21.1155	23.464	22.4881	21.7373	21.053	23.4157	22.482	21.628	21.0469
	Mod.Nei	24.388	23.8718	23.2045	22.7326	24.4283	23.8263	23..2761	22.688	24.3611	23.833	23.159	22.6622
	Proposed K-VSD Wavlet t	25.1334	25.146	24.4782	23.9462	25.4165	24.945	24.9687	25.136	25.2661	24.978	24.568	23.9876
Coif 5	Visushrink	22.5678	19.9391	18.5022	17.5062	22.6137	19.9899	18.4535	17.497	22.6153	19.917	18.486	17.4952
	Neighshrink	26.0778	24.2732	23.1822	22.2243	26.0365	24.3298	23.0888	22.289	26.0615	24.278	23.123	22.2693
	Mod.Nei	27.2788	26.008	25.0155	24.1331	27.2752	26.0147	24.9283	24.161	27.2978	25.981	24.999	24.1564
	Proposed K-VSD Wavlet	30.3458	28.455	29..3464	27.5781	28.3756	29.4655	29.1005	28.489	28.3201	29.0172	28.0756	28.453

Table I Comparative Mammographic image PSNR Values for Proposed (K-VSD) with Novel Threshold Wavelet and Other Existing Methods

| e-ISSN: 2320-9801, p-ISSN: 2320-9798| www.ijircce.com | Impact Factor: 7.194 |

|| Volume 8, Issue 4, April 2020 ||

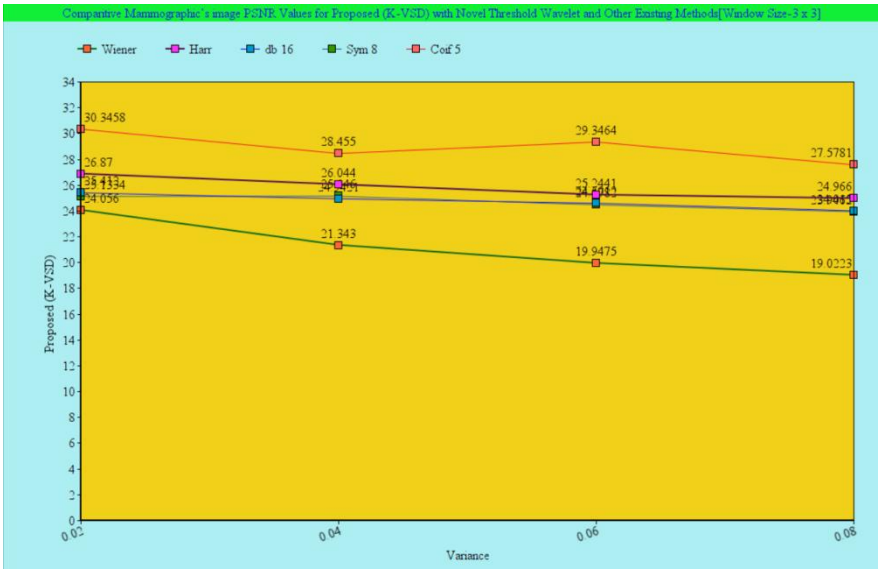

Fig 9 Comparitive Mammographic's image PSNR Values for Proposed (K-VSD)-Window Size:3 x 3

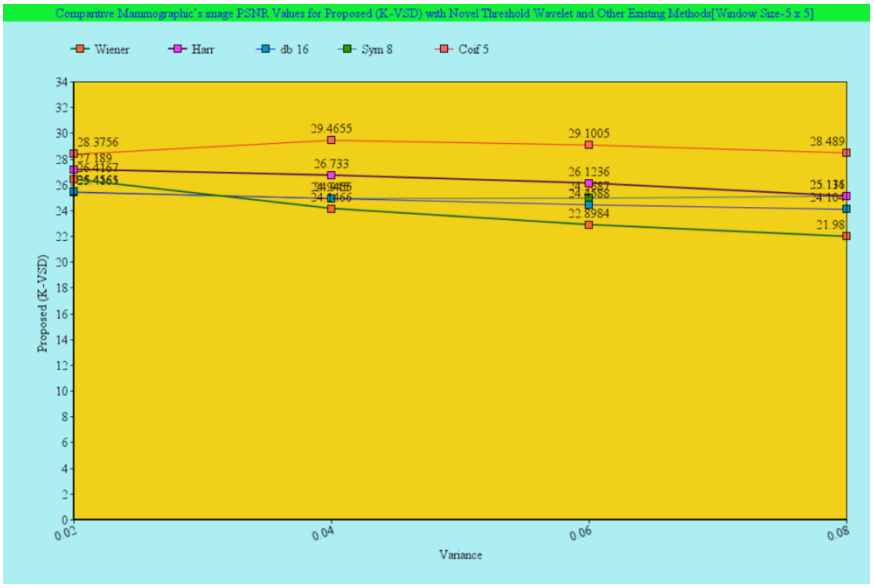

Fig 10 Comparitive Mammographic's image PSNR Values for Proposed (K-VSD)-Window Size:5 x 5

| e-ISSN: 2320-9801, p-ISSN: 2320-9798| www.ijircce.com | Impact Factor: 7.194 |

|| Volume 8, Issue 4, April 2020 ||

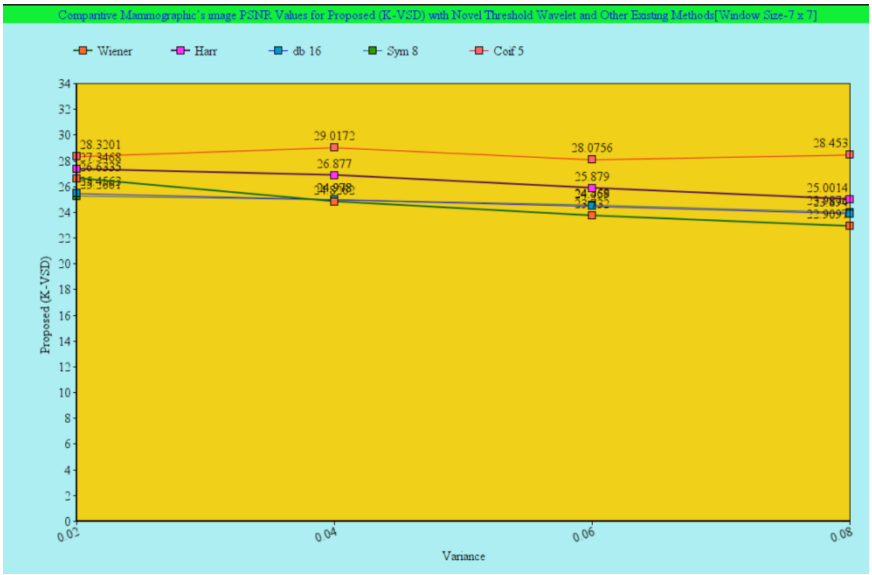

Fig 11 Comparitive Mammographic's image PSNR Values for Proposed (K-VSD)-Window Size:7 x 7

V EVALUATION CRITERIA FOR WAVELET THRESHOLD METHOD

The above said methods are evaluated using the quality measure Peak Signal to Noise ratio which is calculated using the formulae,

$$\text{PSNR} = 10\log_{10}\frac{255^2}{\text{MSE}}\ (\text{db})$$

where MSE is the mean squared error between the original image and the reconstructed de-noised image. It is used to evaluate the different de-noising scheme like Wiener filter, Visushrink, Neighshrink, Modified Neighshrink, wavelet and multi-wavelet for all mamographic images.

VI CONCLUSION

In this paper, an important research challenge is to improve the visual quality of mammograms through image processing in order to detect breast cancer at an early stage. This paper describes new methods for mammographic image preprocessing for noise suppression based on the wavelet transform. The image preprocessing was designed to enhance the local contrast in dense regions adaptively. The image denoising process also is adaptive and the selection of a gain factor provides the desired and detailed enhancement. The preliminary results indicate that our method improves the detection of microcalcifications and other suspicious structures, even in situations where their detection is difficult (e.g. in low contrast image regions, in dense tissues), The experiments were conducted to study the suitability of different wavelet with novel threshold in different window sizes. Experimental results also show that our novel threshold Neighsureshrink method proved best performance compared with Modified Neighshrink, Neighshrink, Weiner filter and Visushrink. Our method requires less user adjustment parameters. Finally, our proposed Novel Threshold method has produced better mammographic screening results for physician for the early detection of breast cancer. And also the proposed method has produced best PSNR values.

REFERENCES

[1] C. Stein, "Estimation of the Mean of a Multivariate Normal Distribution," *Ann. Statist*., 9, 1135–1151, 1981.

[2] D.L. Donoho , "Wavelet Shrinkage and W.V.D A 10 min tour," *Progress Wavelet Anal.*, 1993.

[3] Y. Xu , JB. Weaver, D.M. Healy,and J.Lu , "Wavelet Transform Domain Filters: A Spatially Selective Noise Filtration Technique," *IEEE Transact Image Process.*, Vol. 3, 6, pp.747–58, 1994.

| e-ISSN: 2320-9801, p-ISSN: 2320-9798| www.ijircce.com | Impact Factor: 7.194 |

|| Volume 8, Issue 4, April 2020 ||

[4] D.L. Donoho and I.M. Johnstone, "Ideal Spatial Adaptation via Wavelet Shrinkage," *Biometrika,* 81, 425– 455, 1994.
[5] D.L. Donoho and I.M. Johnstone. "Adapting to Unknown Smoothness via Wavelet Shrinkage," *J. Amer. Statist. Assoc.*, 90, 1200–1224, 1995.
[6] Ep. Simoncelli and Eh. Adelson, "Noise Removal Via Bayesian Coring," *Proceedings Of 3rd IEEE International Conference On Image Processing*, Lausanne, Switzerland, pp. 171– 174, 1996.

[7] G. Bui and Y. Chen, "Translation Invariant De-noising Using Multiwavelets," *IEEE Transactions on Signal Processing*, Vol. 46, No. 12, pp. 3414-3420, 1998.

[8] V. Strela , J. Portilla, and Ep. Simoncelli, "Image Denoising Via A Local Gaussian Scale Mixture Model In The Wavelet Domain", *Proceedings Of The Spie 45th Annual Meeting.* San Diego, Ca; 2000.

[9] T. Blu and F. Luiser, "The Sure-LET Approach to Image Denoising," *IEEE terms, Image Process.,* Vol 16, pp.2778-2786, 2000.

[10] K.Z. Lin, D.P. Li, and K.Q. Hua , "Operator Description of Image Wavelet Denoising," *Journal of Harbin University of Science and Technology*, Vol. 5, pp. 8 -12, 2000.

[11] N. FLS, H. Schiabel,R.H. Benatti,R.C. Stamato, M.C. Escapinati, and C.E. Goes., "A Method to Contrast Enhancement of Digital Dense Breast Images Aimed to Detect Clustered Microcalcifications," *In Proceedings of 9th IEEE International Conference on Image Processing*, Thessaloniki, Greece, pp. 305–8, 2001.

[12] T. T. Cai and B.W. Silverman, "Incorporating Information on Neighbouring Coefficients into Wavelet Estimation," *Sankhya, Ser.*, B 63, 127–148, 2001.
[13] O .O. Gurun, P. Fatouros, G.M. Khun, and E.S. de Paredes, "A Controlled Phantom Study of a Noise Equalization Algorithm for Detecting Microcalcifications in Digital Mammograms," *Medical Physics,* Vol. 28, 4, pp. 445–54, 2001.

[14] L. Sendur and I.W. Selesnick, "Bivariate Shrinkage with Local Variance Eestimation," *IEEE Signal Process. Lett.*, 9, 438–441, 2002a

[15] L. Sendur and I.W. Selesnick, "Bivariate Shrinkage Functions for Wavelet-Based Denoising Exploiting Interscale Dependency", *IEEE Trans Signal Processing*, 2002.

[16] L. Sendur and I.W. Selesnick, "Bi-Variate Shrinkage with Local Variance Estimation," *IEEE Signal Processing Letters*, Vol. 9, No. 12, pp. 438-441, 2002.

[17] P. Bao and L. Zhong, "Noise Reduction for Magnetic Resonance Image via Adaptive Multiscale Products Thresholding," *IEEE transact Medical Image*, 2003.
[18] G.Y. Chen and T.D. Bui, "Multi-Wavelet De-Noising Using Neighboring Coefficients," *IEEE Signal Processing Letters*, Vol. 10, No. 7, pp. 211-214, 2003.

[19] P. Heinlein, J. Drexl, and W. Schneider, "Integrated Wavelets for Enhancement of Microcal Fications in digital mammography." *IEEE Transact Med Imaging*, Vol.22, 3, pp. 402–13, 2003.

[20] I.K. Fodor and C. Kamath, "Denoising Through Wavelet Thresholding: An Empirical Study," *SPIE J. Electron. Imaging*, 12, 151–160, 2003.

[21] G.Y. Chen, T. D. Bui, and A. Krzyzak, "Image Denoising with Neighbour Dependency and Customized Wavelet and Threshold," *Pattern Recognition*, 38, 115–124, 2005.

[22] I.W. Selesnick, R.G. Baraniuk, and N. G. Kingsbury, "The Dual-Tree Complex Wavelet Transform," *IEEE Signal Process. Mag.*, 22, 123–151, 2005.

| e-ISSN: 2320-9801, p-ISSN: 2320-9798| www.ijircce.com | Impact Factor: 7.194 |

|| Volume 8, Issue 4, April 2020 ||

[23] Jacob, Schorconsk, and Claudio rosito Juns, "Denoising and Enhancing Digital Momographic Images for Visual Screeing," *Computerized Medical Imaging and Graphic*, pp. 243-254, 2006.

[24] A. Pizurica and W. Philips, "Estimating Probability of Presence of a Signal of Interest in Multiresolution Single- and Multiband Image Denoising," *IEEE Trans. Image Process.*, 15, 654–665, 2006a.

[25] T. Blu and F. Luisier ," The SURE-LET Approach to Image Denoising," *IEEE Trans. Image Process.* 16, 2778–2786, 2007.

[26] F. Luisier, T. Blu, and M. Unser, "A New SURE Approach to Image Denoising: Interscale Orthonormal Wavelet Thresholding," *IEEE Trans. Image Process.*, 16, 593– 606, 2007a.

[27] Dr.S.Kother Mohideen "Denoising of Images Using Complex Wavelet"International Journal of Advanced Scientific and Technical Research ,ISSUe 2,Volume1 February 2012,ISSN 2249-9954

[28] S. Shajun Nisha1, P. Thazneem Fazila ,Dr. S. Kother Mohideen,"HrperspectralImage Mixed Noise Reduction Based on Improved K-SVD Algorithm", International Journal of Research in Engineering Technology IJRET , Volume: 03 Special Issue: 07 |May-2014, eISSN: 2319-1163 | pISSN: 2321-7308